JTTEE5 18:500–509
DOI: 10.1007/s11666-009-9402-6
1059-9630/$19.00 © ASM International

Peer Reviewed

Effect of Thermal Treatment on High-Temperature Mechanical Properties Enhancement in LPPS, HVOF, and APS CoNiCrAlY Coatings

Hiroyuki Waki, Takeshi Kitamura, and Akira Kobayashi

(Submitted June 19, 2009; in revised form September 18, 2009)

The mechanical properties of a MCrAlY coating significantly influence the initiation of cracks in the superalloy substrate under thermomechanical-fatigue conditions. Previous studies have developed a convenient method for evaluating the mechanical properties of sprayed coatings by lateral compression of a circular tube coating. This method does not need chucking, and manufacturing the free-standing coating is quite straightforward. In this study, the mechanical properties of the free-standing CoNiCrAlY coatings prepared using low-pressure plasma spraying (LPPS), high-velocity oxyfuel (HVOF) spraying, and atmospheric plasma spraying (APS) were systematically measured with the lateral compression method at room temperature through to 920 °C. The effect of postspray thermal treatments, in vacuum and in air, on the mechanical properties was investigated in the 400 to 1100 °C temperature range. It was found that high-temperature thermal treatment in air was effective in increasing the bending strength and Young's modulus. It was especially effective on the APS coatings, which were produced using powders with average size 60 μm, and on HVOF coating, whose bending strengths increased by approximately three times. On the contrary, the enhancement in the LPPS and APS coatings produced with powders 21 μm in size was found to be approximately 1.6 times.

Keywords bending strength, bondcoat, elastic modulus, high-temperature mechanical properties, MCrAlY, thermal barrier coating, thermal treatment

1. Introduction

Thermal barrier coatings (TBCs) and oxidation-resistant coatings are necessary for the protection of superalloy substrates in combustors, blades, and vanes of aircraft engines and power-generation plants. Yttria-stabilized zirconia is commonly used as a TBC on superalloy substrates. Presently, TBCs can be made essentially by two methods: electron beam physical vapor deposition (EBPVD) and plasma spraying (Ref 1). MCrAlY overlay coatings, where M is Co and/or Ni, have been commonly used as oxidation-resistant coatings to protect the superalloy substrates from high-temperature oxidation and corrosion. The MCrAlY coatings are also used as bondcoats to promote the adhesion of TBCs. Presently, the MCrAlYs deposited by low-pressure plasma spraying (LPPS) and high-velocity oxyfuel (HVOF) spraying are used in industrial gas turbine blades and aerospace combustors (Ref 1). It is known that the mechanical properties of a MCrAlY coating significantly influence the initiation of cracks in the superalloy substrate under thermomechanical-fatigue conditions (Ref 2, 3). The mechanical properties of MCrAlY coatings are known to depend on the spraying process and the microstructures significantly (Ref 4-7). It is also known that the properties can be enhanced by the postspray treatment, the temperature of which is above approximately 1000 °C (Ref 8-10). However, the report of high-temperature mechanical properties is not sufficient (Ref 10, 11), because evaluation of high-temperature mechanical properties of the coating is not so easy.

Previous studies have developed a convenient method for evaluating the mechanical properties of sprayed coatings by lateral compression of a circular tube coating (Ref 10, 12, 13). The specimens are freestanding, and the thickness of the coatings is approximately 300 μm. This method does not need chucking, and manufacturing the freestanding coating is quite straightforward. In this article, the dependence of Young's moduli and bending

This article is an invited paper selected from presentations at the 3rd Asian Thermal Spray Conference (ATSC2008) and has been expanded from the original presentation. ATSC2008 was held at Nanyang Executive Centre, Singapore, November 6-7, 2008, and chaired by K.A. Khor.

Hiroyuki Waki, Department of Mechanical Engineering, Osaka Electro-Communication University, 18-8 Hatsu-cho, Neyagawa, Osaka 572-8530, Japan; **Takeshi Kitamura**, Division of Mechanical and Control Engineering, Graduate School of Osaka Electro-Communication University, 18-8 Hatsu-cho, Neyagawa, Osaka 572-8530, Japan; and **Akira Kobayashi**, Joining and Welding Research Institute, Osaka University, 11-1 Mihogaoka, Ibaraki, Osaka 567-0047, Japan. Contact e-mail: waki@isc.osakac.ac.jp.

strengths of the CoNiCrAlY coatings on testing temperature was examined by the lateral compression method. The CoNiCrAlY coatings deposited by three types of spraying method, LPPS, HVOF, and atmospheric plasma spraying (APS) were manufactured. In particular, the effect of postspray thermal treatment on the enhancement of high-temperature mechanical properties was systematically examined.

2. Experimental Method

2.1 Circular Tube Specimen

The circular tube specimen developed by the authors is shown in Fig. 1. Manufacturing procedure was as follows. First, blasting was carried out over the pipe made of mild steel with the thickness of 1 mm. Subsequently, CoNiCrAlY (Co, 32 wt.% Ni, 21 wt.% Cr, 8 wt.% Al, 0.5 wt.% Y) was coated over the pipe using HVOF, LPPS, or APS, as shown in Fig. 1(a). The pipe with the coating was cut to pieces 5 mm long using a diamond disk cutter. The cut surface was polished using #2000 sandpaper. Last, only the mild steel pipe was dissolved out by nitric acid, as shown in Fig. 1(b). It is a great advantage that manufacturing such a freestanding coating specimen is quite straightforward. Residual stress should be taken into account when coating materials. However, the circular tube specimen was freestanding and the stress induced by the substrate was relieved. Furthermore, the specimen did not deflect differently from the conventional plate type of specimens because the shape of the specimen was axially symmetric.

Four kinds of circular tube coatings (Table 1) were manufactured. The APS coatings were classified into a fine coating and a course coating. As-sprayed specimens and thermally treated specimens were prepared. The coatings were thermally treated in the 400 to 1100 °C temperature range in order to investigate the effect of postspray thermal treatment. The thermal treatment consisted of 3 h holding at maximum temperature followed by furnace cooling. Treatment in vacuum was also conducted as well as that in air. These thermal treatments were carried out after dissolving out the substrates. The spraying conditions are shown in Table 2. The thickness of all the coatings was approximately 300 μm.

2.2 Experimental Setup of the Lateral Compression of the Circular Tube

Lateral compression was applied to the circular tube specimen using an electrohydraulic fatigue test machine as shown in Fig. 2. Heating was carried out by induction heating with a radiation thermometer as shown in Fig. 2. The temperature measured by the radiation thermometer was correlated with measurements obtained through thermocouples. The testing temperature ranged from 920 °C to room temperature. The load was measured by the load cell of 500 N. The deformation of the loading plate jig was measured using an eddy current displacement sensor with the resolution of 3 μm.

Table 1 Four kinds of specimens used in this study

	Spraying method	Average spraying powder size, μm
CoNiCrAlY(APS-F)	APS	21
CoNiCrAlY(APS-C)	APS	60
CoNiCrAlY(HVOF)	HVOF	37
CoNiCrAlY(LPPS)	LPPS	21

Table 2 Spraying conditions

	LPPS	APS	HVOF
Equipment	METCO 9 MB	METCO 9 MB	METCO DJ
Arc current, A	500	500	···
Arc voltage, V	60	60	···
Arc Ar, MPa	0.69	0.69	···
Arc H_2, MPa	0.48	0.41	···
O_2, MPa	···	···	0.30
Propylene, MPa	···	···	0.27
Air, MPa	···		0.34
Spraying distance, mm	360	150	150

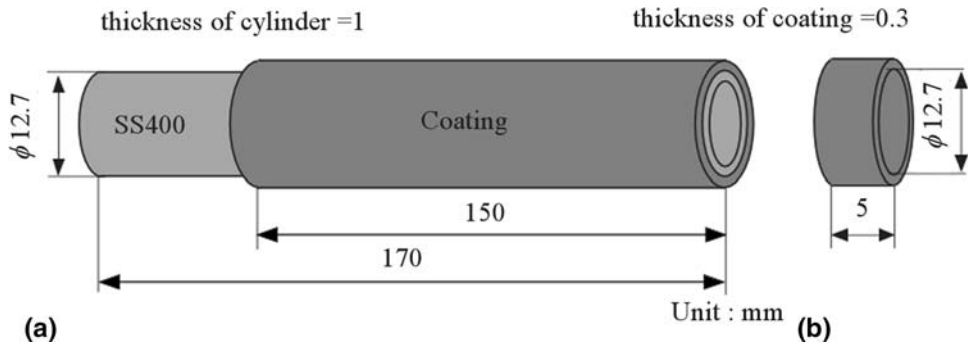

Fig. 1 Manufacturing procedure of the freestanding specimen. (a) As-sprayed coating on the cylindrical substrate made of mild steel. (b) Freestanding coating after dissolved out the substrate by nitric acid

3. Evaluation Theory of Mechanical Properties by Lateral Compression of the Circular Tube

3.1 Young's Modulus

Deformation of the loading plate jig, δ, was measured. The elastic contact with the flat plate jig and the tube surface, δ_{Hz}, should be taken into account as well as the bending of the tube, δ_b, because the δ_{Hz}/δ_b increases with an increase of the thickness of the tube. It was confirmed that Young's moduli of several kinds of well-known materials, mild steel, copper, and brass, obtained from lateral compression tests, agreed with the true values within about 10% error independent of the thickness (Ref 12). In this study, the thickness of the CoNiCrAlY coatings, h, were approximately 300 μm. The deformation of elastic contact need not to be taken into account, because δ_{Hz}/δ_b is lower than about 0.2% when h/R is lower than 0.05, where R is the mean radius of the tube. Young's modulus E is obtained from the curved beam theorem of Eq 1 (Ref 10, 12-14).

$$E = \frac{3\pi R^3}{Lh^3}\left\{1 - H + 2.4(1+\nu)H - \frac{8}{\pi^2}(1-H)^2\right\} \cdot \left(\frac{P}{\delta}\right) \quad \text{(Eq 1)}$$

where (P/δ) is the slope between applied load P and displacement δ, L is length of the tube, and H is defined as $H = h^2/(12R^2)$. The obtained relationship between the load and displacement in elastic deformation should be used for the calculation.

3.2 Bending Strength

One of the most important advantages of the lateral compression of the cylindrical tube specimen is that the specimen fractures in four separate locations. In other words, bending strengths of four locations can be obtained from only one test piece. As shown in Fig. 3, first the tube fractures at inner surface in the vertical direction, point A

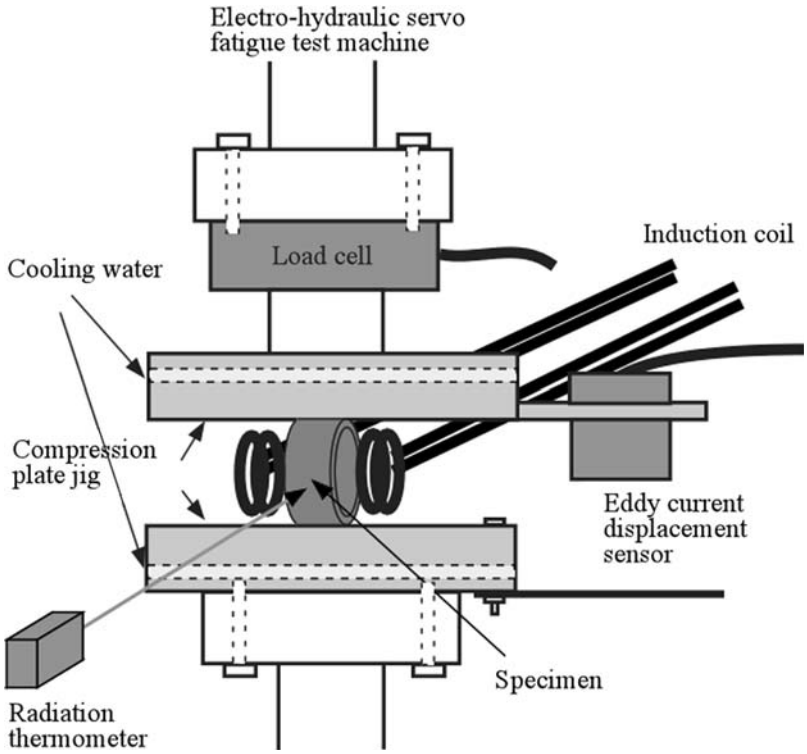

Fig. 2 Experimental setup of the lateral compression of the circular tube specimen

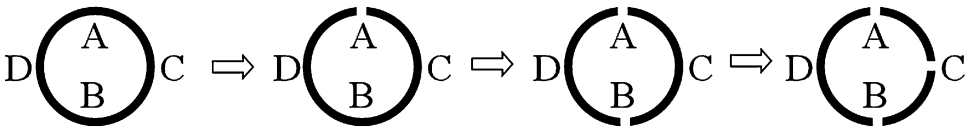

Fig. 3 Fracture process of the lateral compression of the circular tube. The tube fractures at four separate locations in the order of higher stress

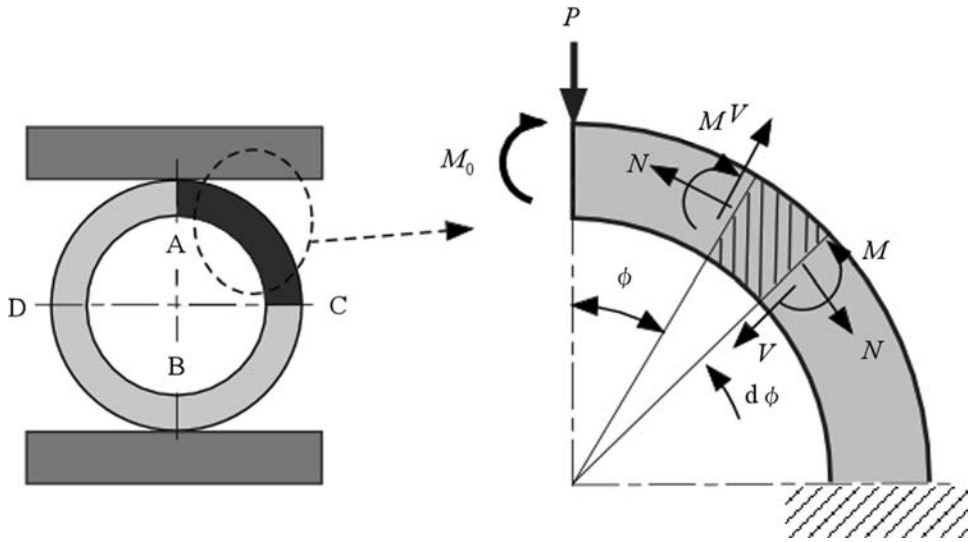

Fig. 4 Model of the lateral compression of the unbroken circular tube

or B. This is because the stresses of point A and B are approximately 1.5 times higher than those of point C and D. The load does not drop to zero because the specimen remains stiff in spite of the fracture. Second, it fractures at another side B or A. The order of fracture at either point A or B is random, because the stresses at point A and B are the same. Subsequently, it fractures at the outer surface in the horizontal direction, point C or D. Finally, it fractures at the other side, D or C. The order of fracture at either point C or D is random. The tube specimen is finally divided into four pieces. The fracture order is governed by the principal stress, and the tube fractures in the order of higher stress.

For example, the unbroken specimen is modeled as shown in Fig. 4. Bending moment, normal force, and shearing force is considered in the model. Stresses at point A and B are written as (Ref 10, 12-14):

$$\sigma_{A,B} = P\frac{R-e}{\pi}\frac{(h/2)-e}{Lhe[R-(h/2)]} \quad \text{(Eq 2)}$$

$$e = R - h\left[\ln\frac{R+(h/2)}{R-(h/2)}\right]^{-1}. \quad \text{(Eq 3)}$$

All the cases of fractured tube, fractured at A, fractured at A and B, fractured at A, B, and C, have been modeled similarly to an unbroken model of Fig. 4, and the equations for evaluating the stresses of the models have been derived (Ref 13). Using the derived equations, four strengths can be obtained from only one test piece. In this study, the bending strength at room temperature was calculated from the fracture loads of four locations. The bending strength at high temperature was evaluated from the first fracture load at point A or B, because unfortunately the temperature of the tube dropped immediately after the first fracture as a result of induction heating. If heating had been furnace heating, the four strengths could all have been obtained at high temperature because the temperature of the specimen would not have dropped.

4. Results and Discussion

4.1 Microstructures of CoNiCrAlY Coatings

Axial sections of the coatings were observed using a scanning electron microscope (SEM). The sections of CoNiCrAlY(APS-F), CoNiCrAlY(APS-C), CoNiCrAlY (HVOF), and CoNiCrAlY(LPPS) are shown in Fig. 5. The coatings with 1050 °C postspray thermal treatment in air are shown in Fig. 6. In addition, the coating was laminated in the vertical direction of the figure. Normal stress was applied in the lateral direction of the figure. As shown in Fig. 5 and 6, the CoNiCrAlY(APS-F) coating microstructure has a lot of oxide, which looks black and dark gray. The black region consists of alumina, and the dark gray region consists of oxides of the other elements, Co, Ni, and Cr, called mixed oxide. On the other hand, the CoNiCrAlY(APS-C) coating has less oxide. The CoNiCrAlY(HVOF) and CoNiCrAlY(LPPS) coatings have almost no oxide.

Table 3 shows the fraction of oxide, the sum of the alumina and the mixed oxide. The oxide content was determined by manual image processing one oxide by one oxide. It is found that the APS coating, which was produced using fine powders, is initially oxidized by approximately 30%. On the contrary, the APS coating produced with coarse powders is oxidized by only approximately 5%. It is also found that thermal treatment makes a remarkable increase of oxidation in the case of CoNiCrAlY(APS-F) coating up to 40%. The fraction of oxide in CoNiCrAlY(HVOF) and CoNiCrAlY(LPPS) coatings is lower than 1.0%.

The thickness of the lamella is also shown in Table 3. It was evaluated by measuring the average thickness of 30 lamellas. It is found that the lamella of CoNiCrAlY (APS-F) is remarkably thinner than that of CoNiCrAlY (APS-C) coating. The precipitations, which were known to be intermetallic compounds β-(Ni,Co)Al (Ref 7), are

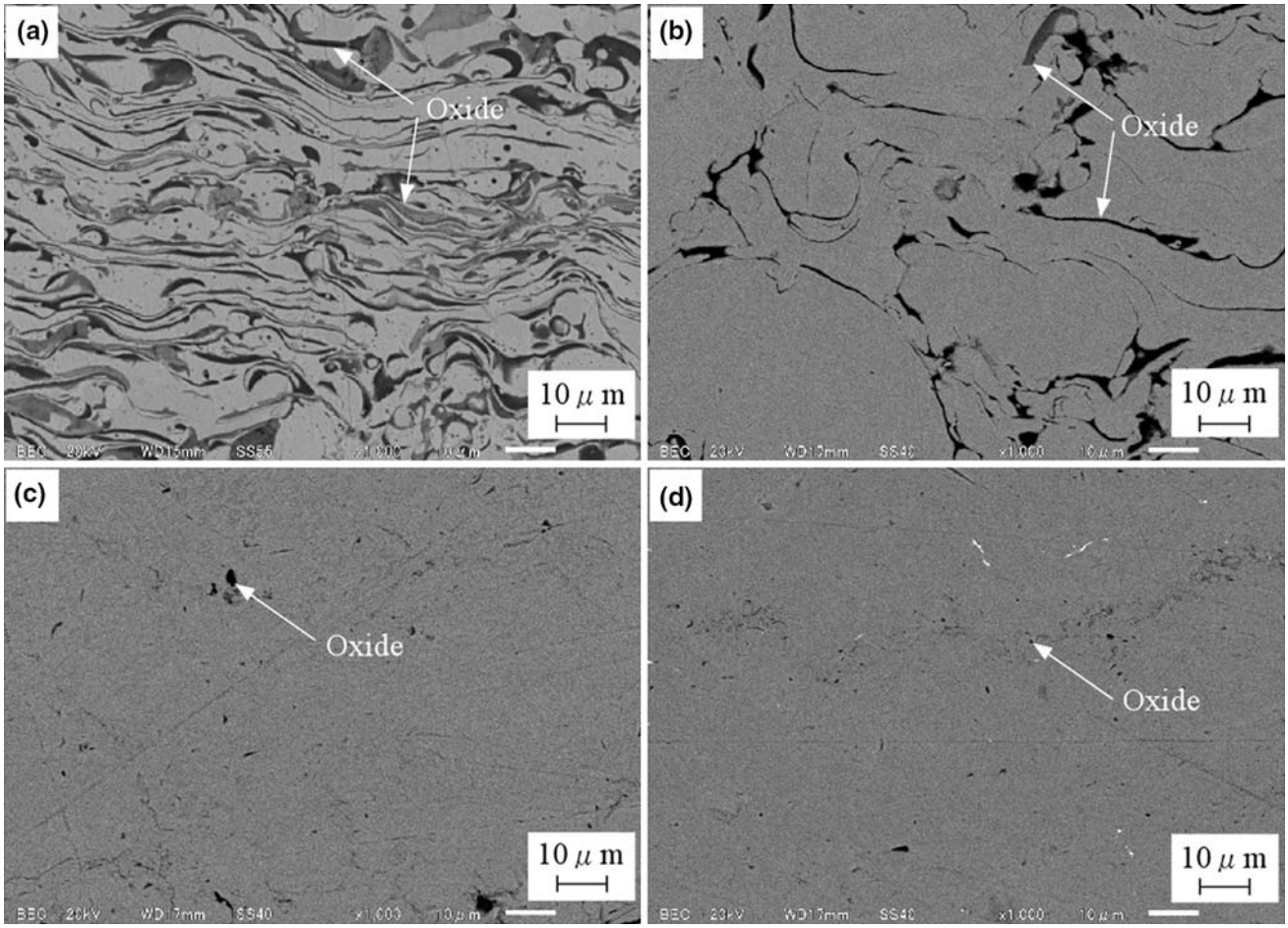

Fig. 5 Scanning electron microscopy images of the as-sprayed specimens. (a) APS-F. (b) APS-C. (c) HOVF. (d) LPPS. The coating was laminated in the vertical direction of the figure. Normal stress was applied in the lateral direction of the figure

observed in CoNiCrAlY(APS-C), CoNiCrAlY(HVOF), and CoNiCrAlY(LPPS) coatings with thermal treatment as shown in Fig. 6. The effect of thermal treatment on the enhancement of high-temperature mechanical properties is compared among the different microstructural coatings in the following sections.

4.2 Relationship Between Load and Displacement of the Circular Tube

The typical relationships between the load per length, P/L, and the displacement, δ, of CoNiCrAlY(APS-F) coatings are shown in Fig. 7(a) to (d). Figures 7(a) and (b) and Fig. 7(c) and (d) show results at room temperature and 590 °C, respectively. Figures 7(a) and (c) and Fig. 7(b) and (d) show the results of as-sprayed coatings and thermally treated coatings at 1050 °C in air, respectively. It is confirmed from Fig. 7(a) and (b) that the test pieces fractured in four separate locations at room temperature. First, the tube fractured at the inner surface in the vertical direction, point A, as shown in Fig. 7(a) and (b). Second, it fractured on the other side at point B. Next, it fractured at the outer surface in the horizontal direction, point C. Finally, it fractured on the other side at point D. The tube specimens finally fractured into four pieces. This method can provide the strengths at four locations from one specimen at room temperature. At high temperature, only the first fracture load was used for evaluation of the bending strength because unfortunately the temperature dropped after the first fracture occurred. Consequently, the loading test was stopped at the first fracture at high temperature as shown in Fig. 7(c) and (d).

The fracture loads, yielding loads, and tangents in the elastic deformation of thermally treated coatings are significantly higher than those of as-sprayed coating at both room and high temperatures as shown in Fig. 7. The effect of postspray thermal treatment and high-temperature mechanical properties are quantitatively described in the following sections.

4.3 Young's Moduli of CoNiCrAlY Coatings

The relationship between Young's modulus of the four types of as-sprayed coatings shown in Table 1 and testing temperature are shown in Fig. 8. The testing temperature is the average of four locations, A, B, C, and D in Fig. 7.

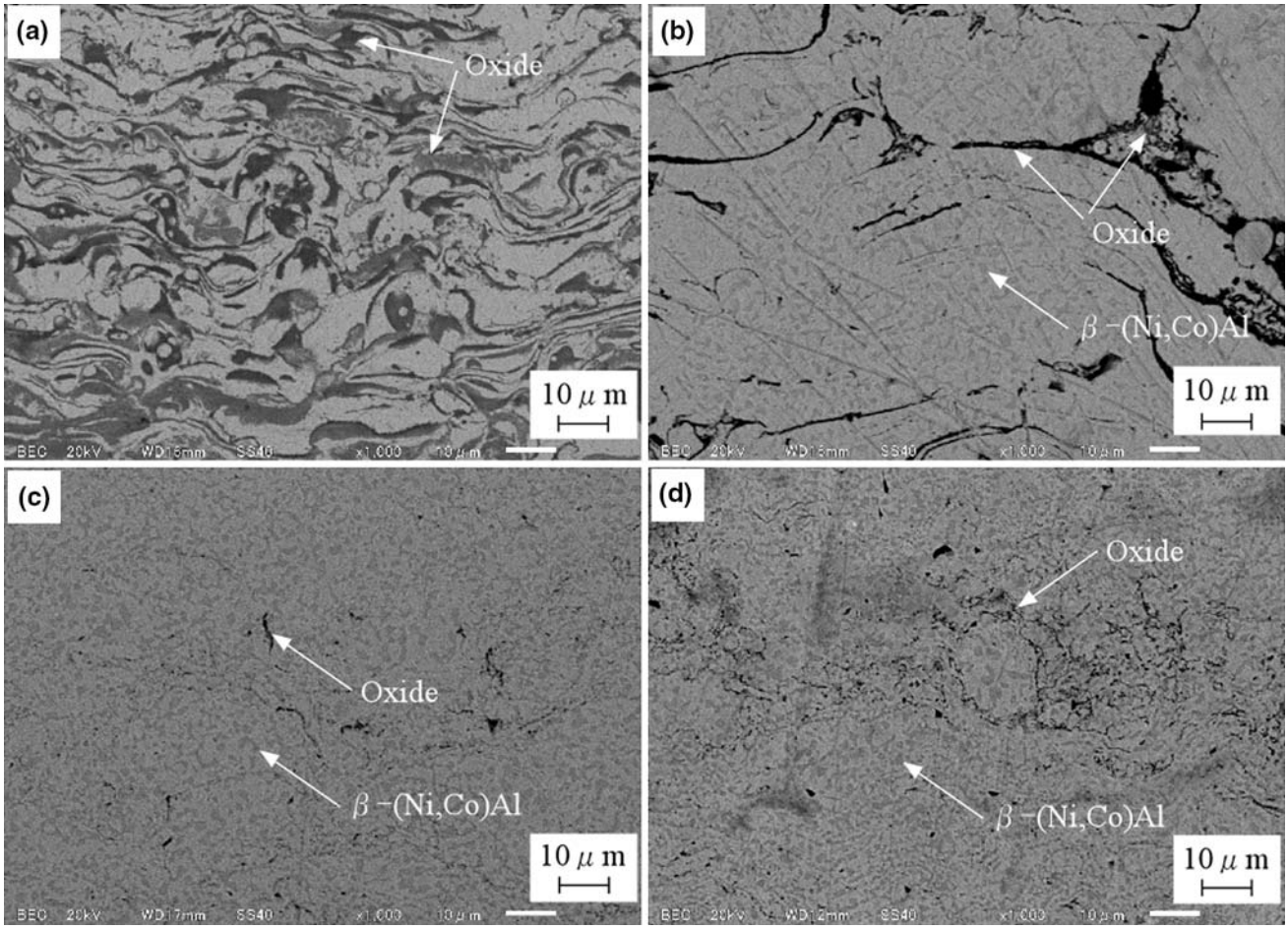

Fig. 6 Scanning electron microscopy images of the specimen with postspray thermal treatment at 1050 °C. (a) APS-F. (b) APS-C. (c) HOVF. (d) LPPS. The coating was laminated in the vertical direction of the figure. Normal stress was applied in the lateral direction of the figure

Table 3 Fraction of oxide and thickness of lamella in the coatings used in this study

Specimen		Fraction of oxide, %	Thickness of lamella, μm
CoNiCrAlY(APS-F)	As-sprayed	29.0	3.0
	Treated	42.3	2.7
CoNiCrAlY(APS-C)	As-sprayed	5.5	11.8
	Treated	5.7	11.0
CoNiCrAlY(HVOF)	As-sprayed	0.29	···
	Treated	0.15	···
CoNiCrAlY(LPPS)	As-sprayed	0.05	···
	Treated	0.85	···

The deformation behavior of plasma sprayed coatings in tension are known to be different from those in compression (Ref 4, 6). The Young's modulus obtained by the lateral compression test was influenced by both tension and compression similarly to the traditional bending test of a plate type specimen. Young's modulus takes a peak value at approximately 400 °C in the case of APS-F, APS-C, and HVOF as shown in Fig. 8. The Young's moduli of the coatings gradually decrease beyond 450 °C. On the contrary, it does not take a peak at 400 °C in the case of LPPS coating. Young's modulus of APS-C coating produced with coarse powders is significantly lower than that of the other coatings, and that of LPPS coating is higher, as shown in Fig. 8. It is well known that microstructure plays an important role in mechanical properties, and high mechanical properties result from a fine microstructure (Ref 4-7).

Figure 9 shows the Young's modulus of thermally treated coatings of APS-F, APS-C, and LPPS plotted against the testing temperature. The data of HVOF coating are shown in a previous article (Ref 10). In the case of APS-F and APS-C coatings, it is found from Fig. 9(a) and (b) that the Young's modulus of the as-sprayed coating is the lowest, and higher thermal treatment enhances the Young's modulus more effectively. It is also found from Fig. 9 that coatings treated in air are have higher Young's modulus than those in vacuum. On the contrary, in the case of LPPS coating, there is no significant difference between as-sprayed coating and thermally treated coatings, as shown in Fig. 9(c).

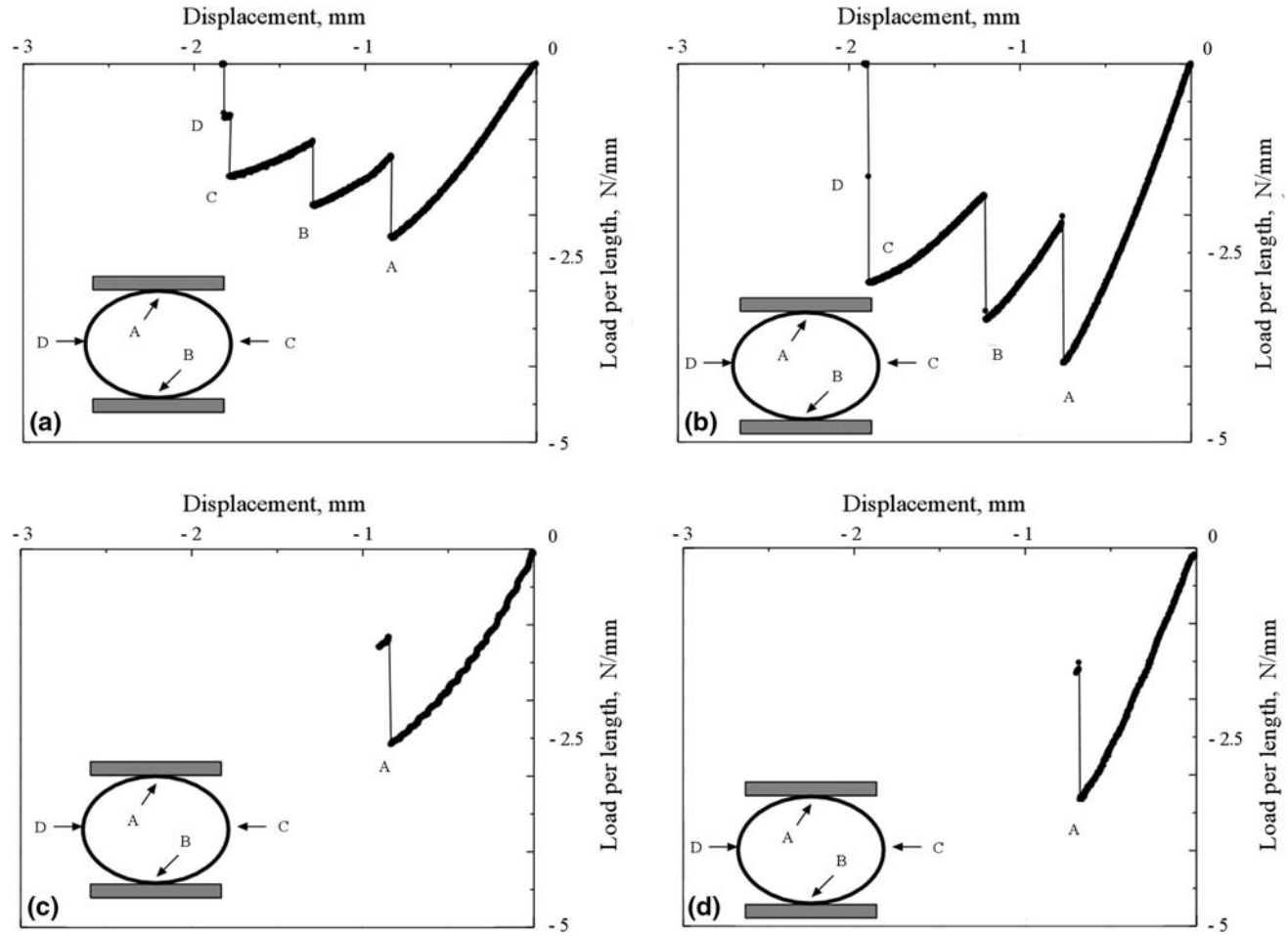

Fig. 7 Typical relationships between the load per length, P/L, and the displacement, δ, of CoNiCrAlY(APS-F) coating. (a) As-sprayed, RT test. (b) 1050 °C treatment in air, RT test. (c) As-sprayed, 590 °C test. (d) 1050 °C treatment in air, 590 °C test

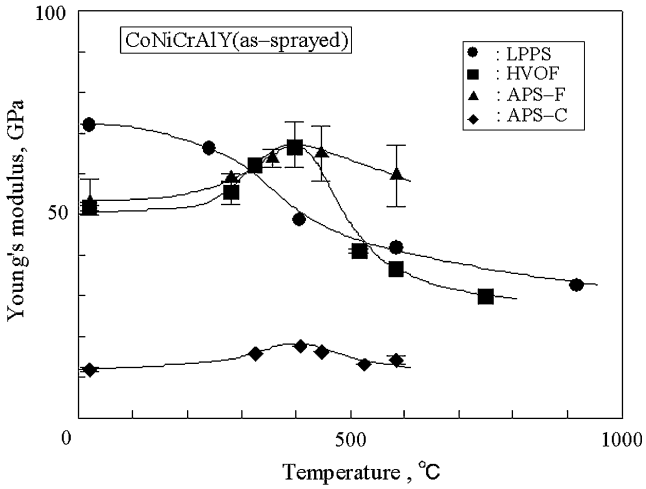

Fig. 8 Young's moduli of four kinds of as-sprayed coatings plotted against the testing temperature

Young's moduli of as-sprayed coatings take a peak value at approximately 400 °C in the cases of APS-F and APS-C coatings as described in first paragraph. On the contrary, those of thermally treated coatings do not take a peak value as shown in Fig. 9(a) and (b). There was the same tendency in the case of the HVOF coating (Ref 10). It was conceived that Young's modulus of as-sprayed coating was enhanced beyond around 400 °C because the high-temperature environment of the loading test was similar to the effect of postspray treatment.

4.4 Effect of Thermal Treatment on Young's Modulus

The effect of postspray thermal treatment is quantitatively examined. Figure 10 shows the enhancement of Young's moduli of four kinds of coatings at room temperature plotted against the temperature of postspray thermal treatment. The vertical axis represents the ratio of Young's modulus of thermally treated coating to that of as-sprayed coating. If the ratio is higher than 1.0, it means the Young's modulus is enhanced. It is found from Fig. 10 that the ratio increases with an increase of the thermal treatment temperature. The APS-C coating shows a particularly rapid increase. On the contrary, the ratio of LPPS coating scarcely changes. It is also confirmed that thermal

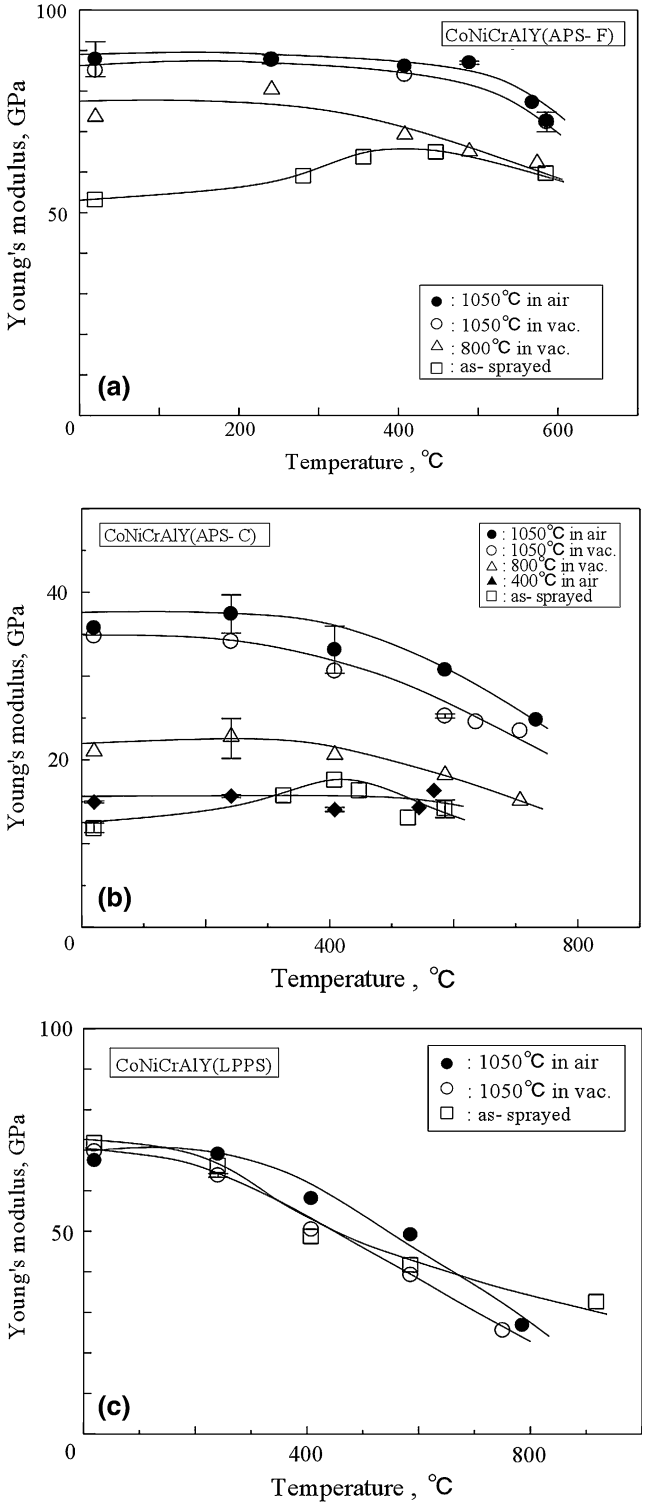

Fig. 9 Young's modulus of thermally treated coatings plotted against the testing temperature. (a) APS-F. (b) APS-C. (c) LPPS

treatment in air is just a little better than that in vacuum. The enhancement of Young's modulus by thermal treatment was evidently primarily caused by the diffusion and sintering of lamella particles because the APS-C coatings

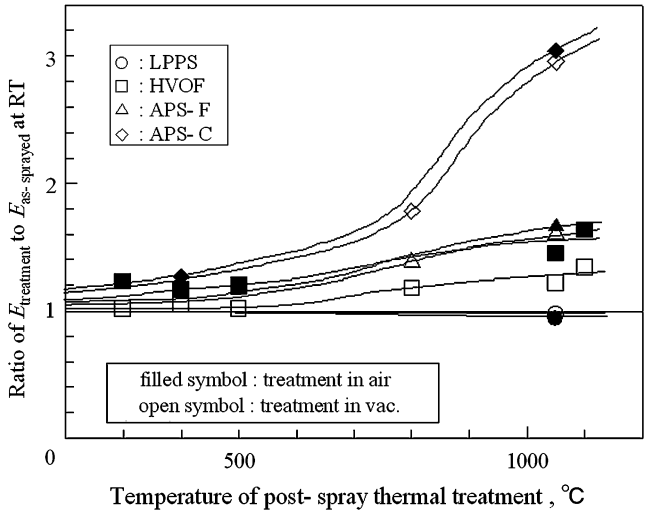

Fig. 10 Improvement of Young's moduli of four kinds of coatings at room temperature plotted against the temperature of postspray thermal treatment

produced with coarse powders showed significant enhancement and LPPS coatings showed insignificant enhancement. It was also evident that precipitation of intermetallic β-(Ni,Co)Al is a secondary factor for the enhancement of Young's modulus because Young's modulus of the APS-F coating without precipitation is more significantly enhanced than that of LPPS coating with precipitation.

4.5 Bending Strengths of CoNiCrAlY Coatings

The relationships between bending strengths of as-sprayed coatings and the testing temperature are shown in Fig. 11. Testing temperature is the value of the fracture location of the specimen. The upward arrows in the figure mean unbroken test data. The bending strengths of the HVOF and LPPS coatings decrease beyond 450 °C, and those of the APS-F and APS-C coatings do not decrease any lower than 500 °C, as shown in Fig. 11. The strength and the Young's modulus of the LPPS coating is the highest and that of the APS-C coating produced with coarse powders is the lowest.

Figure 12 shows the bending strength of thermally treated coatings of APS-F, APS-C, and LPPS plotted against the testing temperature. The data of HVOF coating have been reported in a previous article (Ref 10). It is found that higher thermal treatment enhances the strength as well as the Young's modulus more effectively. The values of coatings treated in air were also higher than those of coatings treated in vacuum. It was conceived that the mechanism of enhancement of bending strength by postspray thermal treatment was similar to that of Young's modulus.

4.6 Effect of Thermal Treatment on Bending Strength

Figure 13 shows the enhancement of bending strength of four kinds of coatings at room temperature plotted

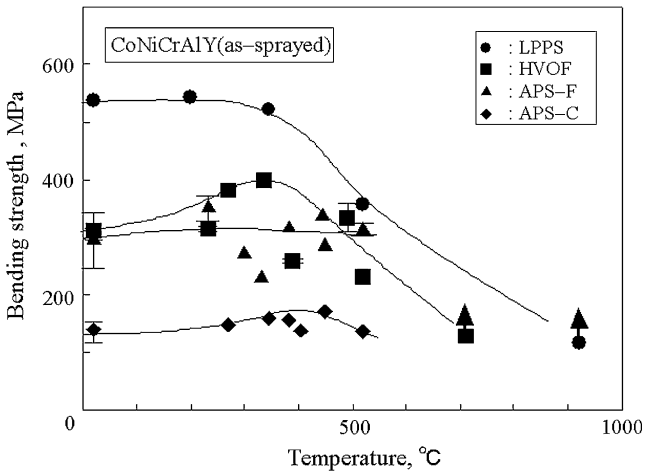

Fig. 11 Bending strength of four kinds of as-sprayed coatings plotted against the testing temperature

against the temperature of postspray thermal treatment. The vertical axis represents the ratio of bending strength of thermally treated coating to that of as-sprayed coating. If the ratio is higher than 1.0, it means the bending strength is enhanced. It is found from Fig. 13 that the ratio increases with an increase of thermal treatment temperature. In particular, HVOF and APS-C coatings show a rapid increase. There was a threshold treatment temperature between 800 and 1050 °C, beyond which the ratio increases rapidly. This agrees with the sintering temperature of CoNiCrAlY. On the contrary, the LPPS coating shows the lowest increase. The enhancement of bending strength by thermal treatment was primarily caused by the diffusion and sintering of laminated and unfused particles, similar to the Young's modulus. It was also evident that precipitation of intermetallic β-(Ni,Co)Al is a secondary factor for the enhancement of bending strength because bending strength of APS-F coating without precipitation is more significantly enhanced than that of LPPS coating with precipitation, similar to the Young's modulus. It is also confirmed that thermal treatment in air is just a little better than that in vacuum, as is Young's modulus.

It was shown that thermal treatment was especially effective on the APS-C coating produced with coarse powders and HVOF coating. It is noted that the strength of thermally treated APS-C coating, of which as-sprayed strength is the lowest, is greater than those of as-sprayed HVOF and APS-F coatings but not higher than that of as-sprayed LPPS coating. In the case of HVOF coating, though the strength of as-sprayed coating is lower than that of as-sprayed LPPS coating, the strength of thermally treated coating is the same as that of thermally treated LPPS coating (Ref 10).

5. Conclusions

The lateral compression method does not need chucking, and manufacturing the free-standing coating is quite

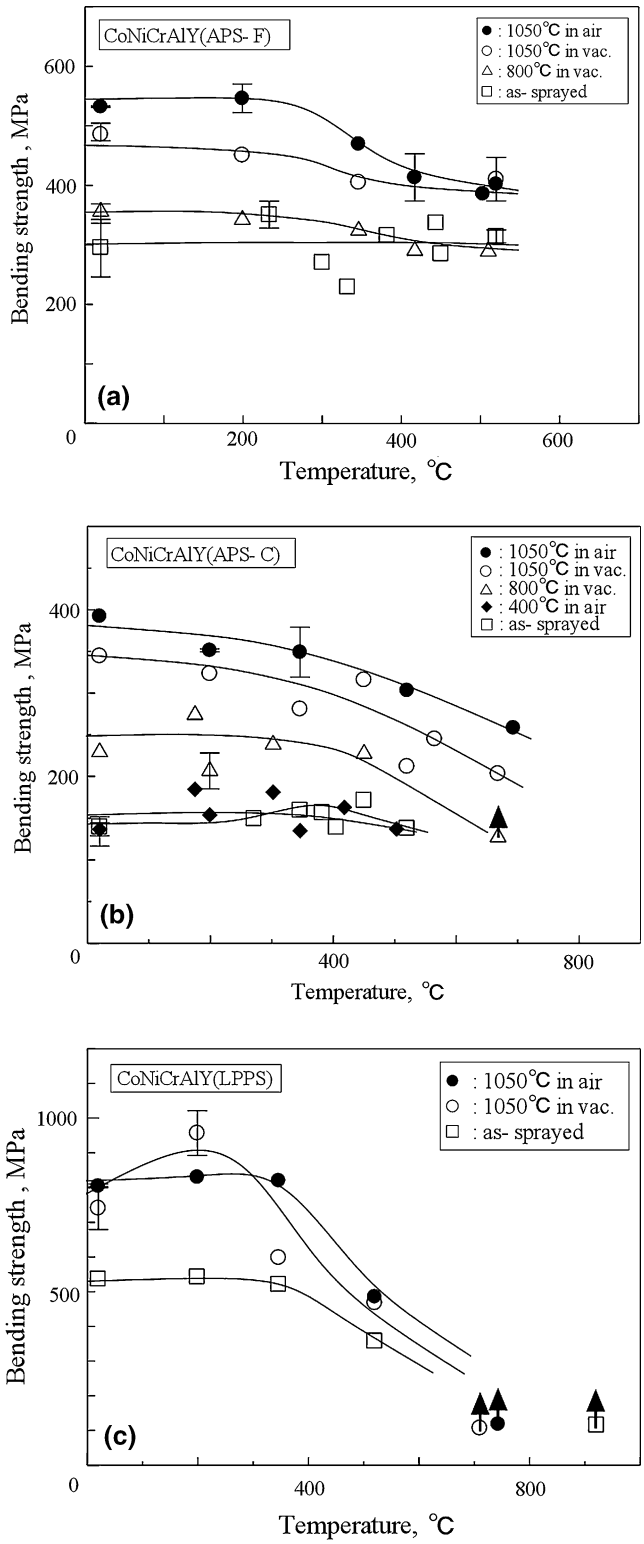

Fig. 12 Bending strength of thermally treated coatings plotted against the testing temperature. (a) APS-F. (b) APS-C. (c) LPPS

straightforward. In this study, the high-temperature mechanical properties of LPPS, HVOF, and APS free-standing CoNiCrAlY coatings were systematically

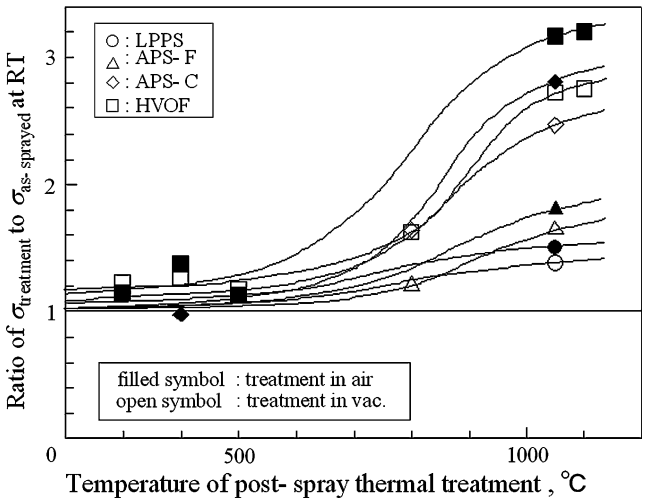

Fig. 13 Improvement of bending strength of four kinds of coatings at room temperature plotted against the temperature of postspray thermal treatment

measured by the lateral compression method. The effect of postspray thermal treatment on the enhancement of mechanical properties was investigated. The results are summarized:

- Young's modulus and bending strength of APS-C coating produced with coarse powders were significantly lower than that of the other coatings, and those of LPPS coating were higher.
- Young's modulus of as-sprayed coatings took a peak value at approximately 400 °C in the case of APS-F, APS-C, and HVOF coatings. On the contrary, the tendency was not observed in the case of LPPS coating. The thermally treated coatings, which took a peak value before thermal treatment, also did not take a peak value.
- Young's modulus and bending strength of the coatings treated in air were higher than those in vacuum in the case of APS-C, APS-F, and HVOF coatings. On the contrary, the tendency was not observed in the case of LPPS coating.
- It was found that high thermal treatment was effective in increasing the bending strength and Young's modulus. It was especially effective on the APS coatings, which were produced using powders with average size 60 μm and on HVOF coating, whose bending strengths increased by approximately three times. On the contrary, the enhancement in the LPPS and APS coatings produced with powders 21 μm in size was found to be approximately 1.6 times.

Acknowledgment

This research has been supported by the Ministry of Education, Science, Sports, and Culture, Grant in Aid for Young Scientists (B), 20760078.

References

1. A. Feuerstein, J. Knapp, T. Taylor, A. Ashary, A. Bolcabage, and N. Hitchman, Technical and Economical Aspects of Current Thermal Barrier Coating Systems for Gas Turbine Engines by Thermal Spray and EBPVD, *J. Therm. Spray Technol.*, 2008, **17**(2), p 199-213
2. M. Okazaki, High-Temperature Strength of Ni-Base Super Alloy Coatings, *Sci. Technol. Adv. Mater.*, 2001, **2**(2), p 357-366
3. H. Waki and A. Kobayashi, Effects of Mechanical Properties of CoNiCrAlY Under-Coating on the High Temperature Fatigue Life of YSZ Thermal Barrier Coating System, *Vacuum*, 2008, **83**(1), p 171-174
4. N. Margadant, J. Neuenschwander, S. Stauss, H. Kaps, A. Kulkarni, J. Matejicek, and G. Rossler, Impact of Probing Volume from Different Mechanical Measurement Methods on Elastic Properties of Thermally Sprayed Ni-Base Coatings on a Mesoscopic Scale, *Surf. Coat. Technol.*, 2006, **200**, p 2805-2820
5. S. Li, C. Langlade, S. Fayeulle, and D. Trehexu, Influence of the Microstructure of Plasma Deposited MCrAlY Coatings on their Tribological Behavior, *Surf. Coat. Technol.*, 1998, **100-101**, p 7-11
6. H. Waki, K. Ogura, I. Nishikawa, and A. Ohmori, Monotonic and Cyclic Deformation Behavior of Plasma-Sprayed Coatings under Uni-Axial Compressive Loading, *Mater. Sci. Eng. A*, 2004, **374**(1-2), p 129-136
7. Y. Itoh and M. Saitoh, Mechanical Properties of Overaluminized MCrAlY Coatings at Room Temperature, *Trans. ASME J. Eng. Gas Turbines Power*, 2005, **127**, p 807-813
8. M. Eskner and R. Sandstrom, Mechanical Properties and Temperature Dependence of an Air Plasma-Sprayed NiCoCrAlY Bondcoat, *Surf. Coat. Technol.*, 2006, **200**, p 2695-2703
9. M. Hasegawa and Y. Kagawa, Microstructural and Mechanical Properties Changes of a NiCoCrAlY Bond Coat with Heat Exposure Time in Air Plasma-Sprayed Y_2O_3-ZrO_2 TBC Systems, *Int. J. Appl. Ceram. Technol.*, 2006, **3**(4), p 293-301
10. H. Waki, K. Nakamura, I. Yamaguchi, and A. Kobayashi, High Temperature Mechanical Properties of Free-Standing HVOF CoNiCrAlY Coatings by Lateral Compression of Circular Tube, *J. Solid Mech. Mater. Eng.*, 2008, **2**(8), p 1161-1171
11. M. Beghini, G. Benamati, L. Bertini, and F. Frendo, Measurement of Coatings' Elastic Properties by Mechanical Methods: Part 2. Application to Thermal Barrier Coatings, *Exp. Mech.*, 2001, **41**(4), p 305-311
12. H. Waki and A. Kobayashi, Development of Lateral Compression Method of Circular Tube Thin Coating for Mechanical Properties of Plasma Sprayed CoNiCrAlY, *Mater. Trans.*, 2006, **47**(7), p 1626-1630
13. H. Waki, Y. Hirota, and A. Kobayashi, Development of Simple and Quadruple Measurement Method for Bending Strengths of Sprayed Coating by Lateral Compression of Circular Tube, *Trans. Jpn. Soc. Mech. Eng. Ser. A*, 2009, **74**(746), p 1342-1350 (in Japanese)
14. S. Timoshenko, *Strength of Materials*, 3rd ed., D. Van Nostrand, Reinhold, NY, 1955, p 381-383